Mathematical Biosciences and Engineering

http://www.aimspress.com/journal/mbe

MBE, 21(4): 5394–5410.
DOI: 10.3934/mbe.2024237
Received: 19 December 2023
Revised: 17 January 2024
Accepted: 26 January 2024
Published: 08 March 2024

Research article

Advancements in health informatics: finite element insights into medial open-wedge high tibial osteotomy and lateral meniscal tears

Lin Chen[1,2,3,†], Mingjun Wang[3,†], Zhanyu Wu[1,2], Jinbo Sun[3], Jianglong Li[3], Chun Chen[3] and Chuan Ye[1,2,*]

[1] Department of Orthopedics, The Affiliated Hospital of Guizhou Medical University, Guiyang 550004, China

[2] Center for Tissue Engineering and Stem Cells, Guizhou Medical University, Guiyang 550004, China

[3] Department of Orthopedics, People's Hospital of Xingyi City, Xingyi 562400, China

† The authors contributed equally to this work.

* **Correspondence:** Email: yechuanchina@hotmail.com.

Abstract: Knee medial compartment osteoarthritis is effectively treated by a medial open-wedge high tibial osteotomy (MOWHTO). The feasibility and safety of MOWHTO for mild lateral meniscal tears are unknown. This study examined the feasibility and safety of knee joint weight-bearing line ratio (WBLr) adjustment during MOWHTO with lateral meniscal injuries. We used a healthy adult male's lower extremities computed tomography scans and knee joint magnetic resonance imaging images to create a normal fine element (FE) model. Based on this model, we generated nine FE models for the MOWHTO operation (WBLr: 40–80%) and 15 models for various lateral meniscal injuries. A compressive load of 650N was applied to all cases to calculate the von Mises stress (VMS), and the intact lateral meniscus' maximal VMS at 77.5% WBLr was accepted as the corrective upper limit stress. Our experimental results show that mild lateral meniscal tears can withstand MOWHTO, while severe tears cannot. Our findings expand the use of MOWHTO and provide a theoretical direction for practical decisions in patients with lateral meniscal injuries.

Keywords: knee osteoarthritis; medial open-wedge high tibial osteotomy; meniscal tears; biomechanics; finite element analysis

1. Introduction

Knee osteoarthritis (KOA) is a prevalent chronic degenerative musculoskeletal disease that predominately occurs in the elderly due to cartilage degradation, synovial membrane inflammation, and hyperosteogenesis [1, 2]. Statistically, KOA affects approximately 33% of people aged 60 years and older, with a staggering disability rate of up to 53% [3], thus imposing a significant health and economic burden [4, 5].

Due to the medial compartment of the knee joint bearing more weight than the lateral compartment, approximately 72% of osteoarthritis cases originate within this compartment [6], accompanied by a shift in the lower extremity weight-bearing line (WBL) to the medial side of the knee joint. A medial open-wedge high tibial osteotomy (MOWHTO) redistributes excessive pressure from the compromised medial compartment to the healthier lateral compartment by correcting the lower extremity WBL, effectively relieving pain, restoring optimal knee joint function, and prolonging joint life, thus making it a highly effective procedure to treat medial compartment osteoarthritis [7, 8]. It involves cutting and repositioning the tibia bone to shift weight away from the damaged part of the knee joint, thereby reducing pressure on the affected area and potentially slowing down the progression of osteoarthritis. MOWHTO is considered important in specific cases where conservative treatments such as physical therapy and medication have not provided adequate relief, and the patient has symptoms of early to mid-stage knee osteoarthritis or issues related to knee alignment. By altering the load distribution within the knee joint, this procedure aims to alleviate pain, improve function, and potentially delay the need for more invasive interventions such as a knee replacement surgery.

MOWHTO has specific indications and contraindications, and the primary criterion is that osteoarthritis is limited to the medial compartment, while the lateral compartment has nondegenerative characteristics with a normal cartilage and meniscus [9, 10]. The decision to undergo MOWHTO should be carefully considered in consultation with a healthcare professional, while taking various factors into account, such as the severity of the condition, the patient's age, activity level, and their overall health. Recent studies have shown that mild degeneration of the lateral compartment does not pose a significant risk of surgical failure [11, 12], thus challenging the traditional view that lateral compartment degeneration automatically disqualifies patients from accepting MOWHTO [13].

While previous studies have separately investigated the biomechanical aspects of MOWHTO correction [14, 15] and meniscal tears [16–18] using a fine element (FE) analysis, there is a lack of research evaluating the simultaneous effects of MOWHTO correction and lateral meniscal tears. In addition, the feasibility and safety of the weight-bearing line ratio (WBLr) correction range when performing MOWHTO in cases of lateral meniscal tears remain unexplored.

In this study, we developed MOWHTO models with WBLr ranging from 40 to 80% and various lateral meniscal tear models to evaluate the stress on a torn lateral meniscus after MOWHTO by a FE analysis. We hypothesize that there is a maximum threshold for the WBLr that would result in too high stress on the lateral meniscus during the performance of a MOWHTO.

2. Materials and methods

2.1. Establishment of three-dimensional models of normal lower extremity and MOWHTO

Precise and comprehensive medical imaging is crucial in various medical diagnostic applications [19, 20], thus providing essential information about different disorders and illnesses [21]. One of the primary steps in utilizing these images for thorough research is the creation of three-dimensional (3D) models [22]. This technique is an initial and essential phase that creates a physical and visual depiction of the internal structures and abnormalities discovered in the medical images [23]. These 3D models serve as a means for physicians and researchers to explore the complexities of anatomical structures [24], thereby facilitating accurate evaluations [25], treatment strategizing [26], and the in-depth analysis necessary to provide effective healthcare solutions [27].

In our study, a computed tomography (CT) scanner (SOMATOM Definition AS Siemens, Germany) captured a series of 976 images with a slice distance of 1 mm, encompassing the hip joint to the ankle joint of a healthy male volunteer (30 years old, 172 cm tall, weighing 65 kg), who had no previous lower extremity injuries. Subsequent magnetic resonance imaging (MRI) scans of the knee joint were conducted, yielding a set of 320 image layers (0.625 mm slice distance) using the MAGNETOM AVanto 3.0 T scanner by Siemens, Germany. Subsequently, all images were inputted into the 3D reconstruction software Mimics 21 (Materialise, Belgium) in the DICOM format; the CT images were utilized to generate 3D bone models, while the MRI images were employed to create 3D models of the cartilage, meniscus, and ligament. Under the guidance of an experienced orthopedist and radiologist, the manual segmentation of non-bony structures was meticulously conducted, with an accuracy level of 0.1 mm. This stringent precision aimed to reduce model variations to the minimum possible extent. The models were exported in the STL format and imported into Geomagic Warp 2021 (Geomagic, USA) for reverse engineering reconstruction. The model's nonuniform rational basis spline (NURBS) surface underwent reconstruction, removal of nails, smoothing, and the subsequent materialization of the surface. Finally, a lower extremity 3D geometric model was generated, and each part was saved in the STEP format.

Then, the STEP format files were imported into Solidworks 2020 (Dassault, USA). As per the established literature [28], the mechanical axis of the lower extremity was identified on the 3D model, which coincided with the weight-bearing line (WBL) (Figure 1(A)). Then, the mechanical lateral distal femur angle (mLDFA, normal: $87 \pm 3^{\circ}$), the mechanical medial proximal tibial angle (mMPTA, normal: $87 \pm 3^{\circ}$), the joint line convergency angle (JLCA, normal: $0 - 2^{\circ}$), the distance between the WBL and the knee joint midpoint (normal: 4 ± 2mm), and the WBL ratio of the knee joint (WBLr, medial: 0%, lateral: 100%) were measured, which confirmed that the established lower extremity model was anatomically completely normal [28] (Figure 1(A)). Based on this model, nine MOWHTO 3D models, with the WBLr ranging from 40 to 80% in 5% increments, were created by modifying the proximal of a normal tibia to the change mMPTA and by repairing the osteotomy gap to simulate the situation of a bone healed after MOWHTO (Figure 1(B)).

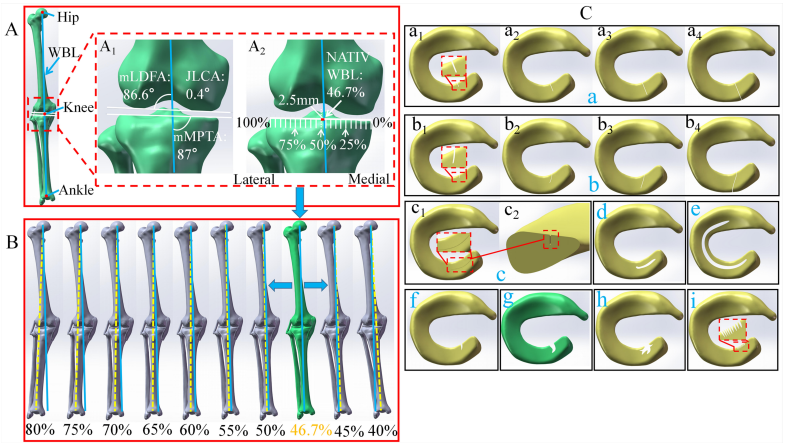

Figure 1. 3D models. (A) Normal lower extremity models, (A_1) Measurement of knee joint anatomical angles, (A_2) Measurement of WBL passing through the knee joint position; (B) MOWHTO models with WBLr from 40 to 80%; (C) Lateral meniscus tears models, (a) Radial tears: (a_1) White zone, (a_2) Red-white zone junction, (a_3) Red zone, (a_4) Complete tear. (b) Oblique tears: (b_1) White zone, (b_2) Red-white zone junction, (b_3) Red zone, (b_4) Complete tear. (c) Partial longitudinal tear. (d) Complete longitudinal tear. (e) Bucket-handle tear. (f) Big oblique tear. (g) Flap tear. (h) Complex tear. (i) Severe degenerative peripheral tear.

2.2. Construction of lateral meniscus anterior horn (LMAH) tear models

The tear model was developed with the lateral meniscus anterior horn (LMAH) as the main focus due to the increased stress on LMAH when standing [15, 16] and the prevalence of LMAH as the most common injury [29]. Referring to the literature [16–18, 30, 31], a total of 15 models of radial and oblique tears in the white zone (radial depth 25%), red-white zone (radial depth 50%), red zone (radial depth 100%), and complete tears (radial depth 100%), as well as partial or complete longitudinal tears, bucket-handle tears, big oblique tears, flap tears, complex tears, and severe degenerative peripheral tears, were created using the Solidworks software (Figure 1(C)).

2.3. FE modeling and material properties

All models were imported into the FEA software, Ansys Workbench 2021 (ANSYS, USA), and meshed using C3D10 elements (Figure 2(A)). Von Mises stress (VMS) tests were performed on the bone, cartilage, and meniscus for the mesh convergence, thus employing a convergence criterion (variation <5%). Finally, the bone mesh size, ligament mesh, meniscus, and cartilage mesh were set to 3, 1.5, 1, and 1 mm, respectively, thus aligning with prior studies [32–34]. On average, each model had approximately 875,000 nodes and 578,500 elements.

Assuming isotropic, homogeneous, and linear elastic behaviors for all models, the Young's modulus (E) values were: cartilage (15 MPa), ligaments (215.3 MPa), meniscus (59 MPa), cortical bone (15000 MPa), cancellous bone (100 MPa); the corresponding Poisson's ratios were 0.475, 0.46, 0.49, 0.3, and 0.3, respectively [17, 33, 35].

2.4. Loads and boundary conditions

Within the assembled model, four sets of non-linear and frictionless contacts were instituted, thus connecting the femoral cartilage with both the medial and lateral menisci, as well as with both the medial and lateral tibial cartilage [32] (Figure 2(B_1)). The posterior and anterior meniscal roots of both the medial and lateral menisci were defined as the 10 mm of meniscal tissue extending downward to the attachment on the tibial plateau within the intercondylar notch, thus simulating the root-meniscal attachment [33] (Figure 2(B_1)). The cartilage-bone and ligament-bone contacts were set to bonded conditions [17, 18, 33, 36]. All six degrees of freedom were restricted for the distal tibia and fibula. Meanwhile, the femur was constrained in flexion-extension, internal-external rotation, and anterior-posterior translation, yet was allowed unrestricted movement in medial-lateral translation and varus-valgus angulation [36]. To apply the "Load", a coordinate system was established, and the Z-direction was consistent with the WBL direction. The weight-bearing surface of the femoral head was selected, a force of 650N, corresponding to a weight of 65 kg, was applied in the Z-direction, and a static analysis of all models was performed using the ANSYS software (Figure 2(B)).

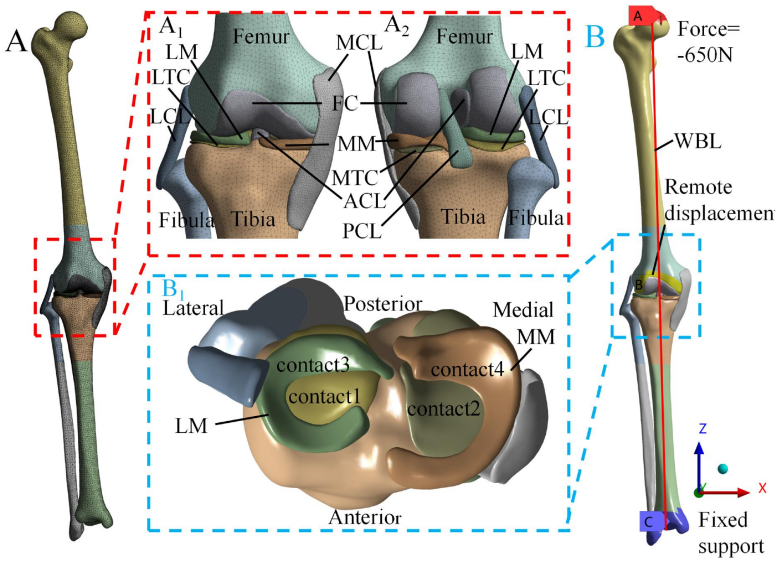

Figure 2. (A) Mesh generation of the lower extremity, (A_1) Anterior view of the right knee, (A_2) Posterior view of the right knee; (B) Loading and boundary condition, (B_1) Top view of the right knee. LM lateral meniscus, MM medial meniscus, ACL anterior cruciate ligament, PCL posterior cruciate ligament, MCL medial collateral ligament, LCL lateral collateral ligament, FC femoral cartilage, LTC lateral tibial cartilage, MTC medial tibial cartilage, WBL weight-bearing line.

2.5. Evaluation indicators

The VMS was the primary assessment parameter to determine the WBLr correction range [37]. Due to the fact that a mechanical tibiofemoral valgus angle greater than 6° (WBLr = 77.5%) may impose excessive stress on the lateral compartment, which ultimately leads to degeneration [38], the maximum VMS in the intact lateral meniscus at a WBLr of 77.5% was the upper limit of stress. One WBLr produced stress on the meniscus that either equaled or exceeded this stress during MOWHTO, which

was the acceptable upper limit WBLr for correction; however, exceeding this value at WBLr ≤ 50% meant that the tear could not undergo MOWHTO. If the value of some tear exceeded the upper limit stress at WBLr of 50 and 55%, no further calculations were performed.

3. Results

3.1. Stress distribution in the intact medial and lateral compartments of the knee joint

The stress load increased in the lateral compartment (with WBLr: 40–80%), while a decrease was observed in the medial compartment (Figures 3(A) and (B)). In the neutral position (WBLr=46.7%), the peak VMS experienced by the lateral meniscus was localized at the anterior horn, measuring 1.01 MPa (Figure 3(C)). Conversely, the medial meniscus exhibited its highest stress at the mid-posterior zone, measuring 1.32 MPa (Figure 3(D)). The stress values for the lateral and medial tibial cartilage were 0.8 and 1.22 MPa (Figures 3(E) and (F)), respectively, with the lateral and medial compartments bearing 39.6 and 60.4% of the total load, respectively. At a WBLr of 55%, both the lateral and medial tibial cartilage experienced a peak VMS of 0.91 MPa, causing a balanced stress distribution between the compartments (Figures 3(B), (E) and (F)). Finally, at a WBLr of 77.5%, the VMS of the lateral meniscus peaked at 1.75 MPa (Figure 3(B)).

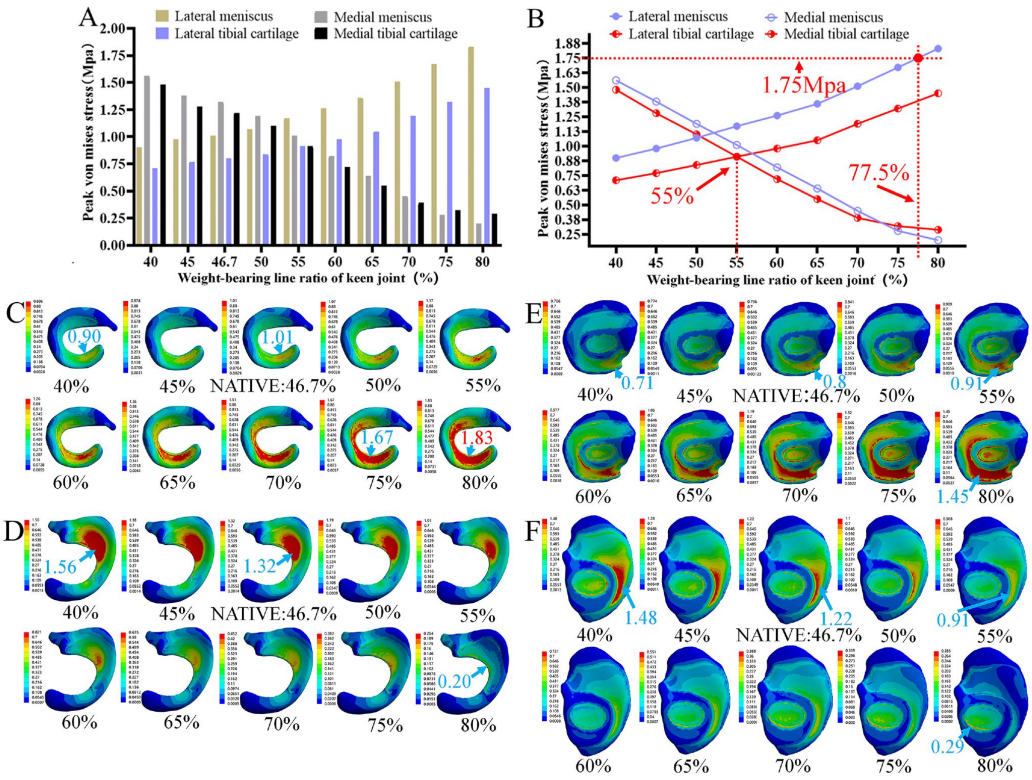

Figure 3. Stress results of the intact knee joint. (A) Peak VMS; (B) Stress distribution in the medial and lateral compartments; (C) Stress cloud map of the lateral meniscus; (D) Stress cloud map of the medial meniscus; (E) Stress cloud map of the lateral tibial cartilage; (F) Stress cloud map of the medial tibial cartilage.

3.2. *Stress distribution in the torn lateral meniscus*

Throughout the range of WBLr variations (40–80%), a consistent linear increase in the peak VMS was observed for all types of lateral meniscus tears (Figures 4(A_2), (B_2), (C_2) and (D_2)). The stress concentration area expanded, with fixed locations of occurrence, which consistently surrounding the fissures (Figures 5–8). When comparing peak VMS values at the same WBLr, the severity order was as follows: white zone tear < red-white zone tear < red zone tear < complete tear for radial tears (Figures 4(A_1) and 5) and oblique tears (Figures 4(B_1) and 6); partial longitudinal tear < complete longitudinal tear (Figures 4(C_1) and 7); and big oblique tear < severe degenerative peripheral tear < flap tear < complex tear (Figures 4(D_1) and 8).

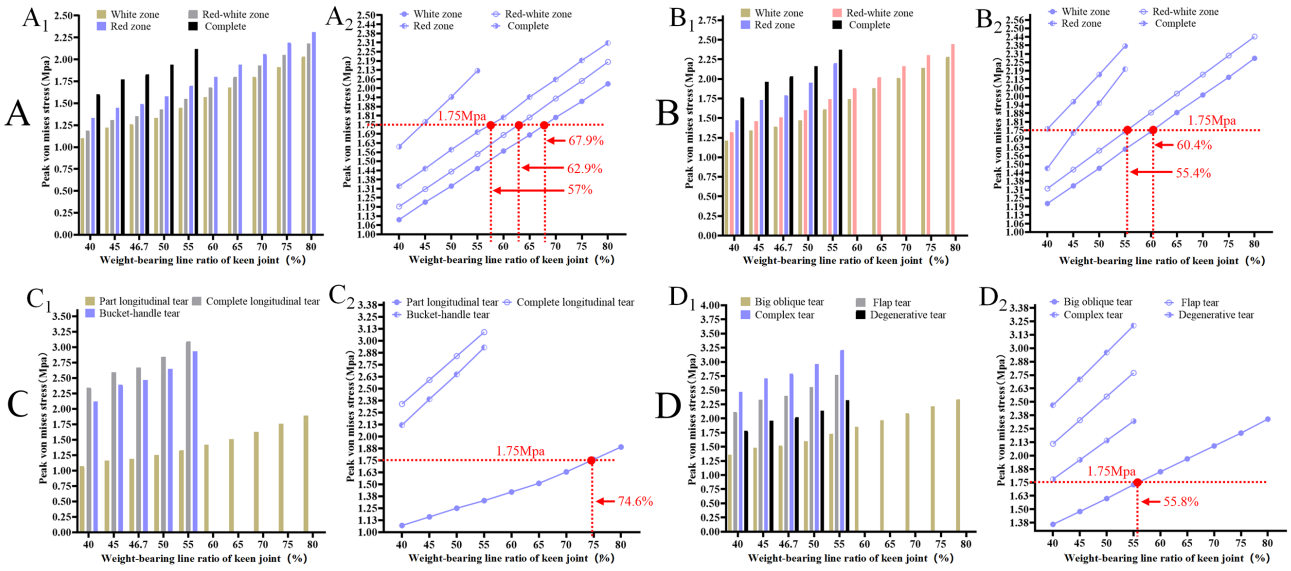

Figure 4. Stress distribution results of different types of meniscus tears (A_1, B_1, C_1, D_1) and acceptable WBLr correction limits(A_2, B_2, C_2, D_2). (A) Radial tears; (B) Oblique tears; (C) Longitudinal tears; (D) Other tears (big oblique tear, flap tear, complex tear, severe degenerative peripheral tear).

3.2.1. Radial tears

For the white zone tear, the peak VMS was 1.68 MPa when the WBLr was 65% and 1.8 MPa when the WBLr was 70% (Figures 4(A_1) and 5(A)), and the corresponding WBLr for a VMS of 1.75 MPa was 67.9% (Figure 4(A_2)). Similarly, for the red-white zone tear, the peak VMS was 1.68 MPa at WBLr = 60%, 1.8 MPa at WBLr = 65% (Figures 4(A_1) and 5(B)), and the corresponding WBLr for a VMS of 1.75 MPa was 62.9% (Figure 4(A_2)). In the case of the red zone tear, the peak VMS was 1.7 MPa when the WBLr was 55% and 1.82 MPa when the WBLr was 60% (Figures 4(A_1) and 5(C)). The corresponding WBLr for a VMS of 1.75 MPa was 57% (Figure 4(A_2)). However, for complete tear, the peak VMS was 1.83 MPa when the WBLr was 46.7%, which exceeded the threshold of 1.75 MPa (Figures 4(A_1) and 5(D)). Therefore, the acceptable WBLr correction limits for the red zone, red-white zone, and white zone radial tears were 57.0, 62.9, and 67.9%, respectively; the complete radial tear

could not be corrected (Figure 4(A_2)).

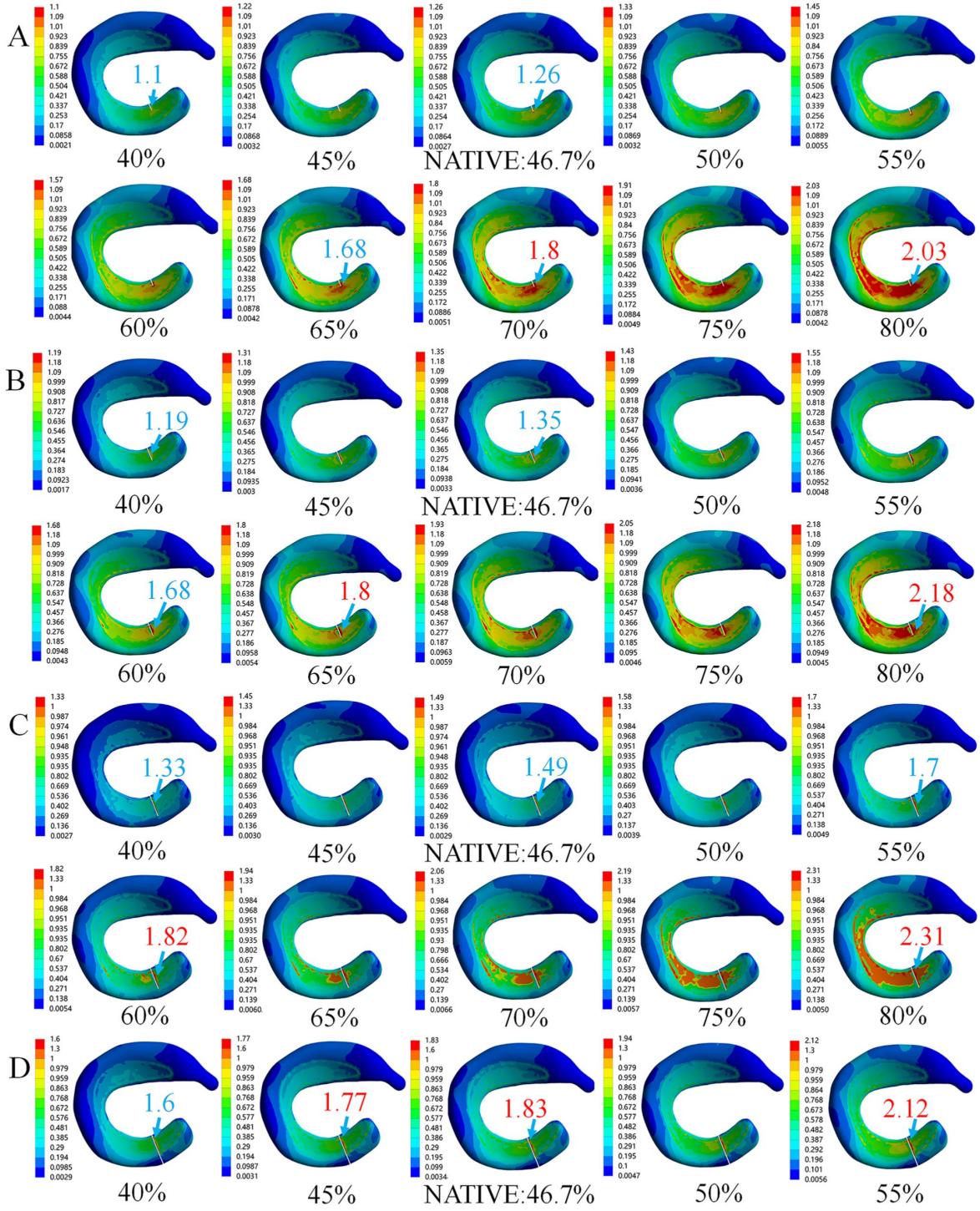

Figure 5. Stress distribution results of meniscus tears of different degrees of radial tears. (A) White zone tear; (B) Red-white zone tear; (C) Red zone tear; (D) Complete tear.

3.2.2. Oblique tears

For the white zone tear, the peak VMS was 1.74 MPa at a WBLr of 60% and 1.88 MPa at a WBLr of 65% (Figures 4(B_1) and 6(A)). The corresponding WBLr for a VMS of 1.75 MPa was 60.4% (Figure 4(B_2)). For the red-white zone tear, the peak VMS was 1.74 MPa at a WBLr of 55% and 1.88 MPa at a WBLr of 60% (Figures 4(B_1) and 6(B)). The corresponding WBLr for a VMS of 1.75 MPa was 55.4% (Figure 4(B_2)). For the red-zone and complete tears, the peak VMS values were 1.79 MPa and 2.03 MPa, respectively, at a WBLr of 46.7%; both values exceeded the threshold of 1.75 MPa (Figures 4(B_1), 6(C), and 6(D)). Consequently, the acceptable WBLr correction limits for the white-zone and red-white zone oblique tears were 60.4 and 57%, respectively, and no correction could be accepted for the red-zone and complete oblique tears (Figure 4(B_2)).

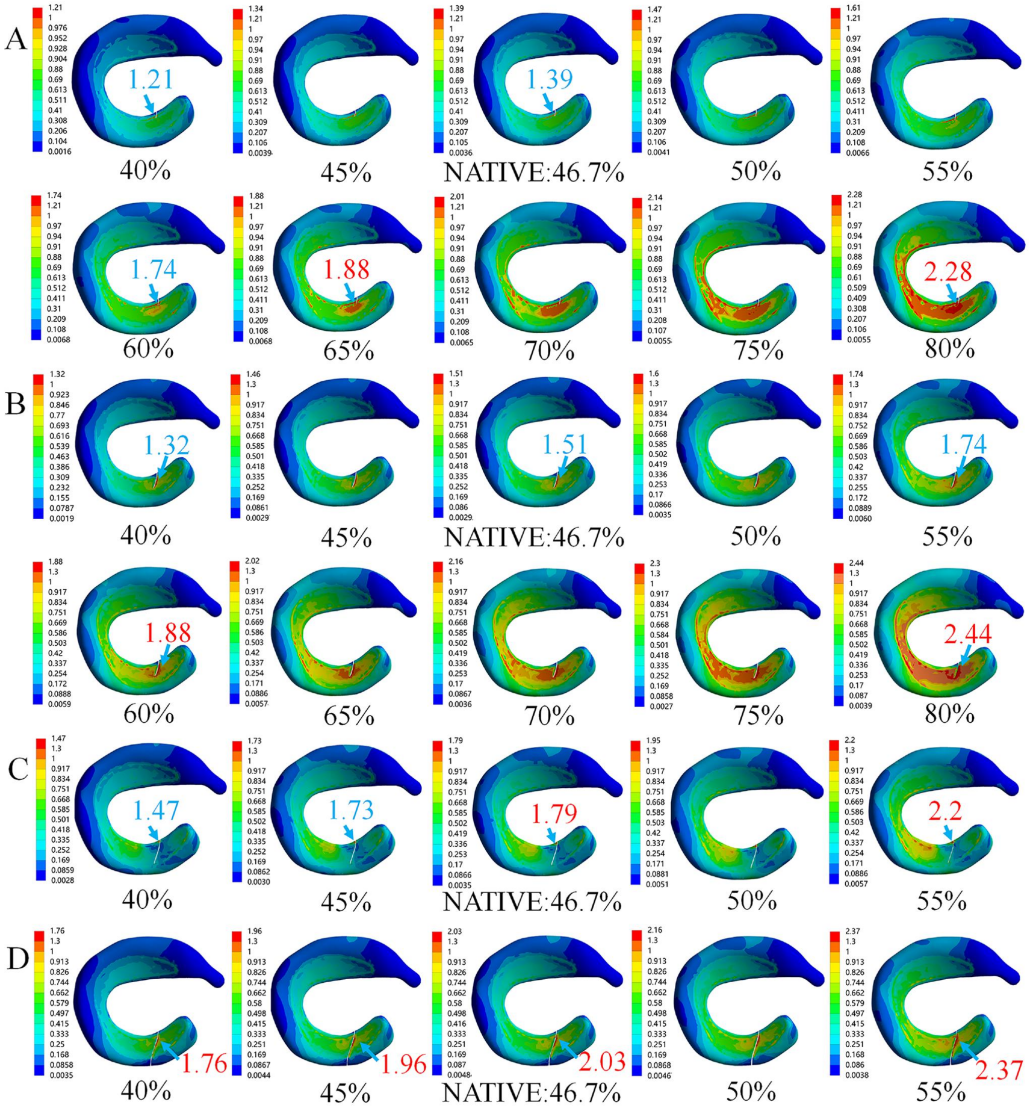

Figure 6. Stress distribution results of meniscus tears of different degrees of oblique tears. (A) White zone tear; (B) Red-white zone tear; (C) Red zone tear; (D) Complete tear.

3.2.3. Longitudinal tears

Partial longitudinal tears exhibited a peak VMS of 1.63 MPa at a WBLr of 70%, which increased to 1.76 MPa at a WBLr of 75% (Figures 4(C_1) and 7A)); a WBLr of 74.6% corresponds precisely to a VMS of 1.75 MPa (Figure 4(C_2)). Alternatively, complete longitudinal and bucket-handle tears demonstrated peak VMS values of 2.67 MPa and 2.47 MPa, respectively, at a WBLr of 46.7%, and both values surpassed the threshold of 1.75 MPa (Figures 4(C_1), 7(B), and 7(C)). Consequently, partial longitudinal tears could withstand a WBLr correction upper limit of 74.6%; the complete longitudinal and bucket-handle tears failed to be corrected (Figure 4(C_2)).

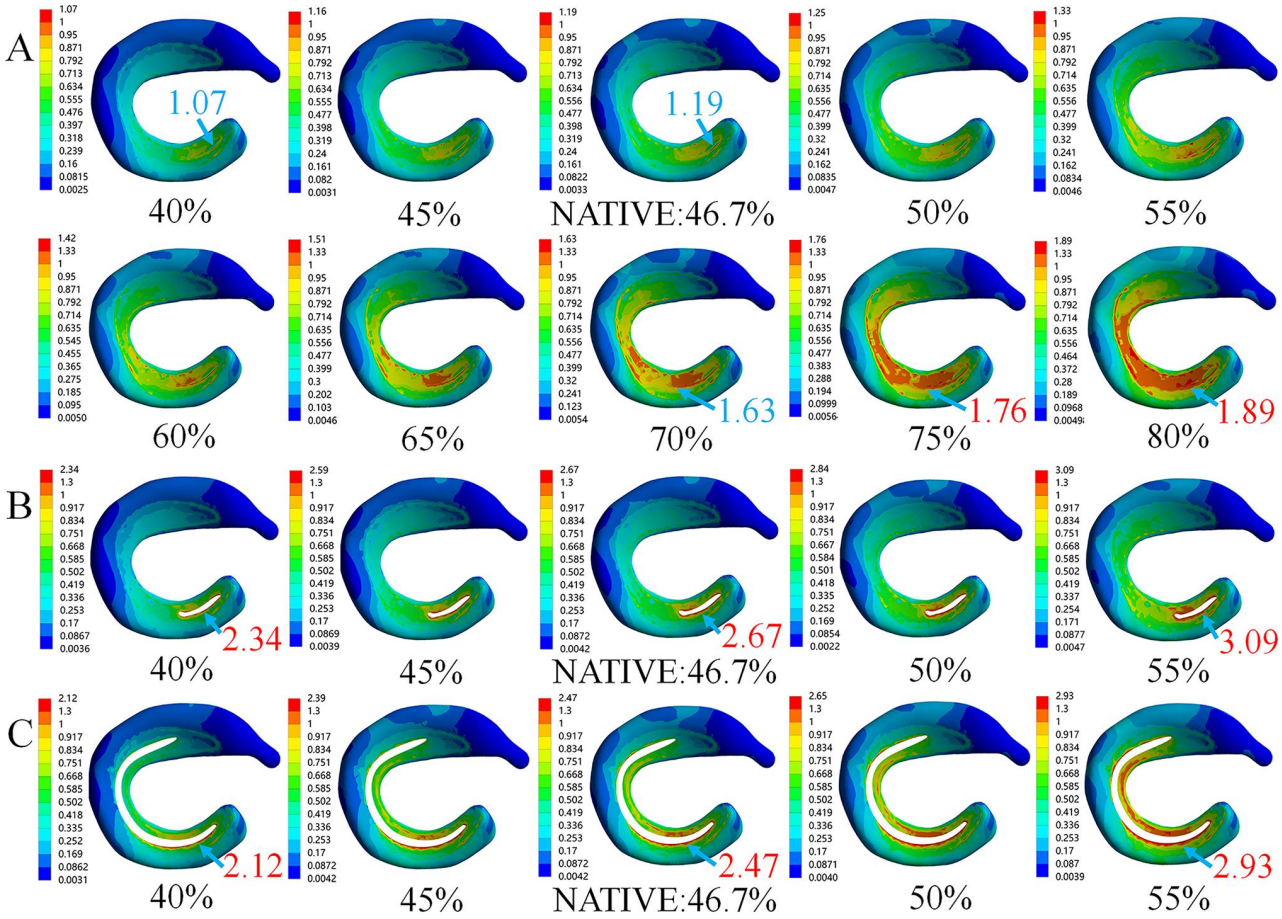

Figure 7. Stress distribution results of meniscus tears of different degrees of longitudinal tears. (A) Partial longitudinal tear; (B) Complete longitudinal tear; (C) Bucket-handle tear.

3.2.4. Other tears

In the case of a big oblique tear, the peak VMS was measured to be 1.73 MPa at a WBLr of 55% and 1.85 MPa at a WBLr of 60% (Figures 4(D_1) and 8(A)). The corresponding WBLr for a VMS of 1.75 MPa was 55.8% (Figure 4(D_2)). As for the flap tear, complex tear, and severe degenerative peripheral tear, the peak VMS values were 2.40, 2.79, and 2.02 MPa, respectively, at a WBLr of 46.7%;

all the values exceeded the threshold of 1.75 MPa (Figures 4(D_1), 8(B), 8(C), and 8(D)). In the case of big oblique tears, the acceptable limit for WBLr correction was 55.8%, and the flap, complex, and severe degenerative peripheral tears were uncorrectable (Figure 4(D_2)).

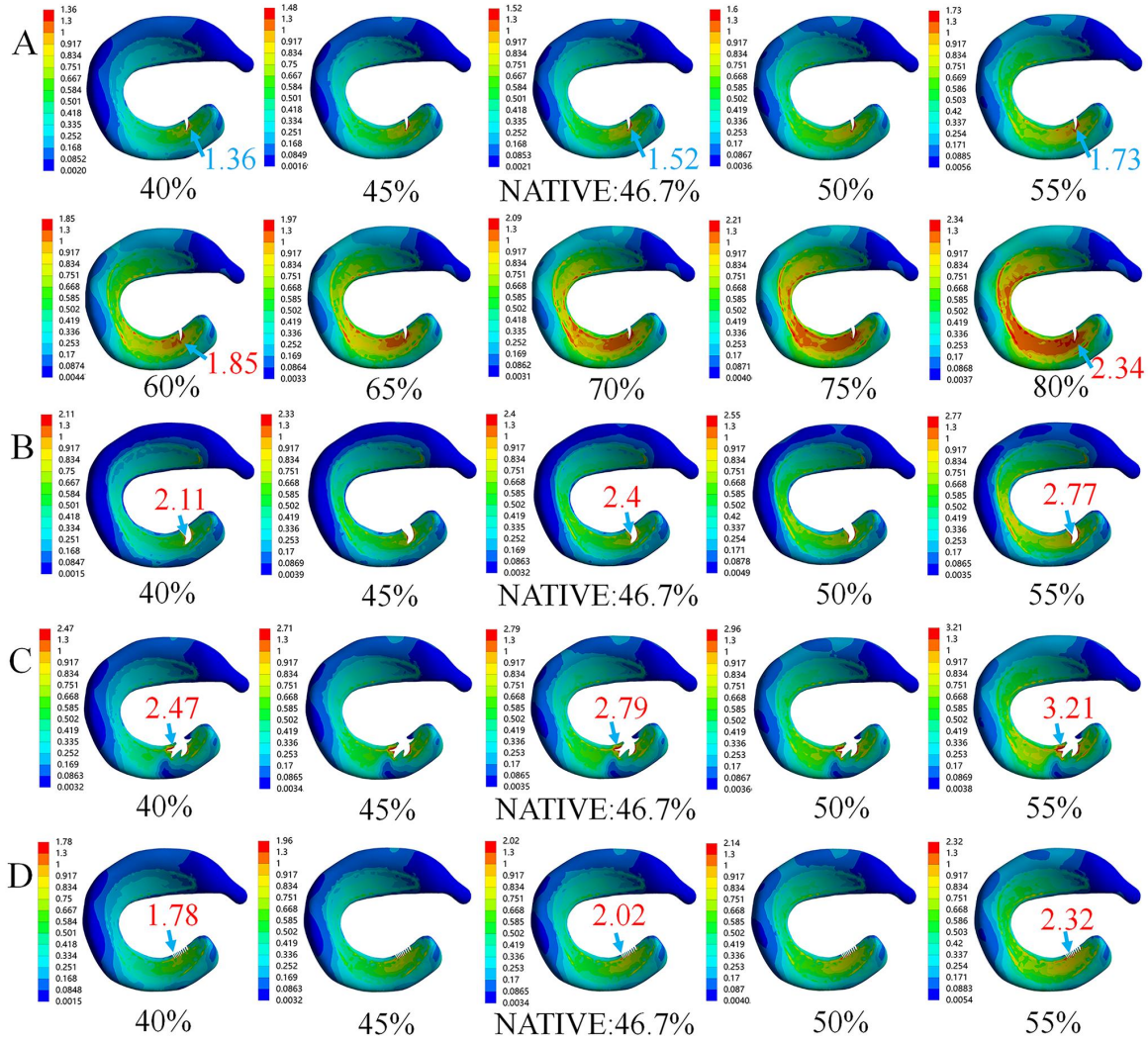

Figure 8. Stress distribution results of meniscus tears of other types. (A) Big oblique tear; (B) Flap tear; (C) Complex tear; (D) Severe degenerative peripheral tear.

4. Discussion

This study successfully developed comprehensive lower extremity FE models to investigate the biomechanical changes associated with lateral meniscal tears when subjected to different WBLr corrections, thus aiming to evaluate the feasibility and safe correction range of conducting MOWHTO in cases involving lateral meniscus tears. The most significant new finding was that mild lateral meniscus tears could withstand varying degrees of WBLr correction. However, as the severity of the tear increased, excessive stress was observed, making the MOWHTO correction inappropriate for severe tear cases, which is consistent with clinical practice.

The accuracy of the FE model employed for knee joint analyses plays a crucial role in determining the research outcomes. Previous studies [33, 34] which investigated normal knee joints using a FE analysis reported higher stress levels in the medial compartment compared to the lateral compartment, while other studies [15, 16] presented contrasting findings. This inconsistency may be attributed to models solely focusing on the knee joint, which neglected the hip and ankle joints and caused deviations in the loading direction concerning the WBL.

To mitigate errors, we developed a comprehensive lower extremity model and a series of lower extremity deformity models with a WBLr correction accuracy of 0.1%. Under a 650 N load applied at a WBLr of 46.7%, the maximum VMS was located in the anterior horn of the lateral meniscus and the mid-posterior region of the medial meniscus, thus aligning with previous findings [15, 16]. Additionally, the load distribution revealed that the lateral and medial compartments supported 39.6% and 60.4% of the total load, respectively, thus aligning with findings documented in literature [15] and the clinical manifestations of medial osteoarthritis [6]. At a WBLr of 55%, the stress distribution in the lateral and medial compartments exhibited a balanced pattern, which agrees with the literature [14]. These findings demonstrate the reliability of the analytical results obtained from the established model and validate its effectiveness.

Meniscal degeneration and tears are recognized as precursors to osteoarthritis and are considered independent risk factors for its development [39]. Clinical studies have shown that increased body weight (stress) contributes to meniscal degeneration [40], which significantly heightens the risk of meniscal tears and secondary osteoarthritis [41, 42]. Our research indicated that both lateral displacement of the WBL and tears increased the stress on the lateral meniscus. Besides, the deeper radial depth of meniscal tears corresponded to a more severe extent and higher stress values. These results align with previous literature [16–18]. Furthermore, the lateral displacement of WBL after MOWHTO will further increase the stress of the meniscus, suggesting tears may worsen, with partial tears progressing to complete tears. The stress redistributed to the lateral compartment after MOWHTO, potentially causing normal meniscal degeneration and susceptibility to tears; in the case of torn menisci, the severity of tears may intensify. Both scenarios contributed to functional meniscus loss, leading to lateral compartment osteoarthritis progression and corrective surgery failure. Our study simulates the process from a healthy to a torn lateral meniscus after MOWHTO, thus offering insight into the biomechanical mechanisms of lateral compartment osteoarthritis following MOWHTO.

The degree of WBL correction is an essential factor affecting the efficacy of MOWHTO. This correction is commonly assessed using either the mechanical tibiofemoral angle or the WBLr [43], which are used interchangeably. In our study, when the mechanical tibiofemoral valgus angle was 6°, the WBLr was 77.5%, which is similar to what has been reported in the literature [44, 45]. It is generally accepted that during MOWHTO, a valgus angle greater than 6° may impose excessive stress on the lateral compartment, thus leading to degeneration [38]. However, the specific stress values associated with this condition remained unclear [46]. We quantified this stress value, and the maximum VMS of the lateral meniscus was 1.75 MPa at a valgus angle of 6° (WBLr = 77.5%); therefore, 1.75 MPa was used as the acceptable upper limit stress for correction in our study.

From a biomechanical standpoint, our study provides the first validation of the feasibility of performing MOWHTO in cases of a lateral meniscal tear and establishes an upper limit for WBLr correction. Specifically, we found that radial tears (white zone, red-white zone, and red zone), oblique

tears (white zone and red-white zone), partial longitudinal tears, and big oblique tears can tolerate WBLr corrections up to 67.9, 62.9, 57.0, 60.4, 55.4, 74.6, and 55.8%, respectively. However, complete tears (radial and oblique), red-zone oblique tears, bucket-handle tears, flap tears, complex tears, and severe degenerative peripheral tears are unsuitable for MOWHTO, as they already experience unacceptably high stress at WBLr=46.7% (neutral position) in our model. This is consistent with the clinical practice that these tears typically require surgical intervention, with either an arthroscopic meniscus repair suture or meniscoplasty being the preferred approach. Moreover, our findings suggest that correcting the deformity may be necessary to reduce stress and facilitate meniscus repair if lateral meniscal tears are accompanied by valgus deformity. Additionally, for tears tolerating WBLr correction near 55% (e.g., red zone radial tear (57%), red-white zone oblique tear (55.4%), and big oblique tear (55.8%)), a simultaneous arthroscopic meniscus repair during MOWHTO could potentially further reduce meniscal stress, increase the WBLr correction limit, and enhance a surgeons' confidence in performing MOWHTO in patients with concomitant lateral meniscal tears.

Although our study challenges the conventional notion that lateral meniscal tears are unsuitable for HTO, it is essential to acknowledge certain limitations. First, all material properties were assumed to be isotropic, linearly elastic, and homogeneous across the models to ensure consistency and prevent bias. However, uniform settings were applied to all models to avoid discrepancies. Second, the models were solely subjected to static loading, thereby omitting the reproduction of joint kinetics during motion. Third, our analysis focused on stress changes in computational models. Robust support for our findings could be obtained through biomechanical tests on human cadaver samples and reliable retrospective clinical observational studies. Finally, our study employed a WBLr in 5% increments, which may be more accurate if refined. However, the study's conclusions should remain unchanged since stress rises linearly.

5. Conclusions

In conclusion, the acceptable WBLr correction upper limits when performing MOWHTO for radial tears (white zone, red-white zone, and red zone), oblique tears (white zone and red-white zone), partial longitudinal tears, and big oblique tears were 67.9, 62.9, 57, 60.4, 55.4, 74.6, and 55.8%, respectively. However, complete tears (radial and oblique), bucket-handle, flap, complex, and severe degenerative peripheral tears could not undergo MOWHTO. Our findings enhance the understanding of the biomechanical mechanisms underlying lateral compartment osteoarthritis after MOWHTO, broaden the application of MOWHTO, and provide a rationale for clinical decisions when conducting MOWHTO in patients with lateral meniscal tears.

Use of AI tools declaration

The authors declare they have not used Artificial Intelligence (AI) tools in the creation of this article.

Acknowledgments

This study was supported by the Department of Science and Technology of Guizhou Province ([2020]6013), the Health Commission of Guizhou Province (gzwkj[2021]-258), The Affiliated Hospital of Guizhou Medical University (gyfynsfc[2022]-19), and the Science and Technology Bureau of Qianxinan Prefecture ([2019]2-63).

Conflict of interest

The authors declare there is no conflict of interest.

References

1. L. N. Reynard, M. J. Barter, Osteoarthritis year in review 2019: Genetics, genomics and epigenetics, *Osteoarthritis Cartilage*, **28** (2020), 275–284. http://doi.org/10.1016/j.joca.2019.11.010
2. D. J. Hunter, S. Bierma-Zeinstra, Osteoarthritis, *Lancet*, **393** (2019), 1745–1759. http://doi.org/10.1016/S0140-6736(19)30417-9
3. J. W. Bijlsma, F. Berenbaum, F. P. Lafeber, Osteoarthritis: an update with relevance for clinical practice, *Lancet*, **377** (2011), 2115–2126. http://doi.org/10.1016/S0140-6736(11)60243-2
4. Q. Liu, S. Wang, J. Lin, Y. Zhang, The burden for knee osteoarthritis among Chinese elderly: estimates from a nationally representative study, *Osteoarthritis Cartilage*, **26** (2018), 1636–1642. http://doi.org/10.1016/j.joca.2018.07.019
5. S. Safiri, A. Kolahi, E. Smith, C. Hill, D. Bettampadi, M. A. Mansournia, et al., Global, regional and national burden of osteoarthritis 1990–2017: A systematic analysis of the Global Burden of Disease Study 2017, *Ann. Rheum. Dis.*, **79** (2020), 819–828. http://doi.org/10.1136/annrheumdis-2019-216515
6. J. C. Stoddart, O. Dandridge, A. Garner, J. Cobb, R. J. van Arkel, The compartmental distribution of knee osteoarthritis-a systematic review and meta-analysis, *Osteoarthritis Cartilage*, **29** (2021), 445–455. http://doi.org/10.1016/j.joca.2020.10.011
7. C. Jacquet, F. Gulagaci, A. Schmidt, A. Pendse, S. Parratte, J. Argenson, et al., Opening wedge high tibial osteotomy allows better outcomes than unicompartmental knee arthroplasty in patients expecting to return to impact sports, *Knee Surg. Sports Traumatol. Arthroscopy*, **28** (2020), 3849–3857. http://doi.org/10.1007/s00167-020-05857-1
8. A. Agarwalla, D. R. Christian, J. N. Liu, G. H. Garcia, M. L. Redondo, A. B. Yanke, et al., Return to work following isolated opening wedge high tibial osteotomy, *Cartilage*, **12** (2021), 468–474. http://doi.org/10.1177/1947603519852417
9. M. Loia, S. Vanni, F. Rosso, D. Bonasia, M. Bruzzone, F. Dettoni, et al., High tibial osteotomy in varus knees: Indications and limits, *Joints*, **4** (2016), 98–110. http://doi.org/10.11138/jts/2016.4.2.098
10. B. Zampogna, S. Vasta, R. Papalia, Patient evaluation and indications for osteotomy around the knee, *Clin. Sports Med.*, **38** (2019), 305–315. http://doi.org/10.1016/j.csm.2019.02.011

11. D. H. Kim, S. C. Kim, J. S. Yoon, Y. S. Lee, Are there harmful effects of preoperative mild lateral or patellofemoral degeneration on the outcomes of open wedge high tibial osteotomy for medial compartmental osteoarthritis?, *Orthop. J. Sports Med.*, **8** (2020). http://doi.org/10.1177/2325967120927481
12. C. Jin, E. Song, A. Santoso, P. S. Ingale, I. Choi, J. Seon, Survival and risk factor analysis of medial open wedge high tibial osteotomy for unicompartment knee osteoarthritis, *J. Arthroscopic Relat. Surg.*, **36** (2020), 535–543. http://doi.org/10.1016/j.arthro.2019.08.040
13. R. S. Khakha, H. R. B. A. Razak, K. Kley, R. van Heerwaarden, A. J. Wilson, Role of high tibial osteotomy in medial compartment osteoarthritis of the knee: Indications, surgical technique and outcomes, *J. Clin. Orthop. Trauma*, **23** (2021), 101618. http://doi.org/10.1016/j.jcot.2021.101618
14. J. L. Martay, A. J. Palmer, N. K. Bangerter, S. Clare, A. P. Monk, C. P. Brown, et al., A preliminary modeling investigation into the safe correction zone for high tibial osteotomy, *Knee*, **25** (2018), 286–295. http://doi.org/10.1016/j.knee.2017.12.006
15. Z. Trad, A. Barkaoui, M. Chafra, J. M. R. Tavares, Finite element analysis of the effect of high tibial osteotomy correction angle on articular cartilage loading, in *Proceedings of the Institution of Mechanical Engineers, Part H: Journal of Engineering in Medicine*, **232** (2018), 553–564. http://doi.org/10.1177/0954411918770706
16. Y. Dong, G. Hu, Y. Dong, Y. Hu, Q. Xu, The effect of meniscal tears and resultant partial meniscectomies on the knee contact stresses: a finite element analysis, *Comput. Methods Biomech. Biomed. Eng.*, **17** (2013), 1452–1463. http://doi.org/10.1080/10255842.2012.753063
17. L. Li, L. Yang, K. Zhang, L. Zhu, X. Wang, Q. Jiang, Three-dimensional finite-element analysis of aggravating medial meniscus tears on knee osteoarthritis, *J. Orthop. Transl.*, **20** (2020), 47–55. http://doi.org/10.1016/j.jot.2019.06.007
18. P. Jiang, J. Cui, Z. Chen, Z. Dai, Y. Zhang, G. Yi, Biomechanical study of medial meniscus after posterior horn injury: a finite element analysis, *Comput. Methods Biomech. Biomed. Eng.*, **23** (2020), 127–137. http://doi.org/10.1080/10255842.2019.1702167
19. B. P. Nguyen, C. Chui, S. Ong, S. Chang, An efficient compression scheme for 4-D medical images using hierarchical vector quantization and motion compensation, *Comput. Biol. Med.*, **41** (2011), 843–856. http://doi.org/10.1016/j.compbiomed.2011.07.003
20. Q. H. Nguyen, B. P. Nguyen, M. T. Nguyen, M. C. H. Chua, T. T. T. Do, N. Nghiem, Bone age assessment and sex determination using transfer learning, *Expert Syst. Appl.*, **200** (2022), 116926. http://doi.org/10.1016/j.eswa.2022.116926
21. X. Chen, B. P. Nguyen, C. Chui, S. Ong, An automatic framework for multi-label brain tumor segmentation based on kernel sparse representation, *Acta Polytech. Hung.*, **14** (2017). http://doi.org/10.12700/aph.14.1.2017.1.3
22. S. Lu, B. Yang, Y. Xiao, S. Liu, M. Liu, L. Yin, et al., Iterative reconstruction of low-dose CT based on differential sparse, *Biomed. Signal Process. Control*, **79** (2023), 104204. http://doi.org/10.1016/j.bspc.2022.104204
23. L. Cai, W. Tay, B. P. Nguyen, C. Chui, S. Ong, Automatic transfer function design for medical visualization using visibility distributions and projective color mapping, *Comput. Med. Imaging Graphics*, **37** (2013), 450–458. http://doi.org/10.1016/j.compmedimag.2013.08.008

24. Y. Xu, F. Zhang, W. Zhai, S. Cheng, J. Li, Y. Wang, Unraveling of advances in 3D-printed polymer-based bone scaffolds, *Polymers*, **14** (2022), 566. http://doi.org/10.3390/polym14030566
25. S. Su, J. He, C. Wang, F. Gao, D. Zhong, P. Lei, A new dressing system reduces the number of dressing changes in the primary total knee arthroplasty: A randomized controlled trial, *Front. Surg.*, **9** (2022). http://doi.org/10.3389/fsurg.2022.800850
26. Y. Miao, X. Wang, S. Wang, R. Li, Adaptive switching control based on dynamic zero-moment point for versatile hip exoskeleton under hybrid locomotion, *IEEE Trans. Ind. Electron.*, **70** (2023), 11443–11452. http://doi.org/10.1109/TIE.2022.3229343
27. Y. Chen, J. Xiang, Z. Wang, Y. Xiao, D. Zhang, X. Chen, et al., Associations of bone mineral density with lean mass, fat mass, and dietary patterns in postmenopausal chinese women: A 2-year prospective study, *PLOS ONE*, **10** (2015), 0137097. http://doi.org/10.1371/journal.pone.0137097
28. N. M. Luís, R. Varatojo, Radiological assessment of lower limb alignment, *Efort Open Rev.*, **6** (2021), 487–494. http://doi.org/10.1302/2058-5241.6.210015
29. D. M. Allen, L. Li, M. D. Crema, M. D. Marra, A. Guermazi, B. T. Wyman, et al., The relationship between meniscal tears and meniscal position, *Ther. Adv. Musculoskeletal Dis.*, **2** (2010), 315–323. http://doi.org/10.1177/1759720X10383198
30. M. E. Wells, J. P. Scanaliato, J. C. Dunn, E. J. Garcia, Meniscal injuries: Mechanism, classification, *Sports Med. Arthroscopy Rev.*, **29** (2021), 154–157. http://doi.org/10.1097/JSA.0000000000000311
31. P. Beaufils, R. Becker, S. Kopf, O. Matthieu, N. Pujol, The knee meniscus: management of traumatic tears and degenerative lesions, *Efort Open Rev.*, **2** (2017), 195–203. http://doi.org/10.1302/2058-5241.2.160056
32. K. Ding, W. Yang, H. Wang, S. Zhan, P. Hu, J. Bai, et al., Finite element analysis of biomechanical effects of residual varus/valgus malunion after femoral fracture on knee joint, *Int. Orthop.*, **45** (2021), 1827–1835. http://doi.org/10.1007/s00264-021-05039-9
33. H. R. C. Bao, D. Zhu, G. S. Gu, H. Gong, The effect of complete radial lateral meniscus posterior root tear on the knee contact mechanics: a finite element analysis, *J. Orthop. Sci.*, **18** (2013), 256–263. http://doi.org/10.1007/s00776-012-0334-5
34. T. Kozaki, D. Fukui, E. Yamamoto, D. Nishiyama, M. Yamanaka, A. Murata, et al., Medial meniscus extrusion and varus tilt of joint line convergence angle increase stress in the medial compartment of the knee joint in the knee extension position-finite element analysis-, *J. Exp. Orthop.*, **9** (2022). http://doi.org/10.1186/s40634-022-00490-y
35. C. Pan, X. Wang, L. Ding, X. Zhu, W. Xu, L. Huang, The best position of bone grafts in the medial open-wedge high tibial osteotomy: A finite element analysis, *Comput. Methods Programs Biomed.*, **228** (2023), 107253. http://doi.org/10.1016/j.cmpb.2022.107253
36. A. E. Kedgley, T. Saw, N. A. Segal, U. N. Hansen, A. M. J. Bull, S. D. Masouros, Predicting meniscal tear stability across knee-joint flexion using finite-element analysis, *Knee Surg. Sports Traumatol. Arthroscopy*, **27** (2019), 206–214. http://doi.org/10.1007/s00167-018-5090-4

37. Y. Wu, X. Jin, X. Zhao, Y. Wang, H. Bai, B. Lu, et al., Computer-aided design of distal femoral osteotomy for the valgus knee and effect of correction angle on joint loading by finite element analysis, *Orthop. Surg.*, **14** (2022), 2904–2913. http://doi.org/10.1111/os.13440

38. B. Ollivier, P. Berger, C. Depuydt, H. Vandenneucker, Good long-term survival and patient-reported outcomes after high tibial osteotomy for medial compartment osteoarthritis, *Knee Surg. Sports Traumatol. Arthroscopy*, **29** (2020), 3569–3584. http://doi.org/10.1007/s00167-020-06262-4

39. M. Englund, A. Guermazi, S. L. Lohmander, The role of the meniscus in knee osteoarthritis: A cause or consequence?, *Radiol. Clin.*, **47** (2009), 703–712. http://doi.org/10.1016/j.rcl.2009.03.003

40. J. B. Guimaraes, M. C. Nevitt, C. E. McCulloch, B. J. Schwaiger, A. S. Gersing, L. Facchetti, et al., Association of weight change with progression of meniscal intrasubstance degeneration over 48 months: Data from the Osteoarthritis Initiative, *Eur. Radiol.*, **28** (2017), 953–962. http://doi.org/10.1007/s00330-017-5054-y

41. M. A. Wesdorp, S. M. Eijgenraam, D. E. Meuffels, S. M. A. Bierma-Zeinstra, G. Kleinrensink, Y. M. Bastiaansen-Jenniskens, et al., Traumatic meniscal tears are associated with meniscal degeneration, *Am. J. Sports Med.*, **48** (2020), 2345–2352. http://doi.org/10.1177/0363546520934766

42. R. J. Ward, J. B. Driban, J. W. MacKay, T. E. McAlindon, B. Lu, C. B. Eaton, et al., Meniscal degeneration is prognostic of destabilzing meniscal tear and accelerated knee osteoarthritis: Data from the osteoarthritis initiative, *J. Orthop. Res.*, **41** (2023), 2418–2423. http://doi.org/10.1002/jor.25575

43. J. Moore, L. Mychaltchouk, F. Lavoie, Applicability of a modified angular correction measurement method for open-wedge high tibial osteotomy, *Knee Surg. Sports Traumatol. Arthroscopy*, **25** (2016), 846–852. http://doi.org/10.1007/s00167-015-3954-4

44. K. Briem, D. K. Ramsey, W. Newcomb, K. S. Rudolph, L. Snyder-Mackler, Effects of the amount of valgus correction for medial compartment knee osteoarthritis on clinical outcome, knee kinetics and muscle co-contraction after opening wedge high tibial osteotomy, *J. Orthop. Res.*, **25** (2007), 311–318. http://doi.org/10.1002/jor.20326

45. Y. Yin, S. Li, R. Zhang, J. Guo, Z. Hou, Y. Zhang, What is the relationship between the "fujisawa point" and postoperative knee valgus angle? A theoretical, computer-based study, *Knee*, **27** (2020), 183–191. http://doi.org/10.1016/j.knee.2019.10.018

46. X. Liu, Z. Chen, Y. Gao, J. zhang, Z. Jin, High tibial osteotomy: Review of techniques and biomechanics, *J. Healthcare Eng.*, **2019** (2019), 8363128. http://doi.org/10.1155/2019/8363128